Proceedings Paper:
Etarhouni, M, Chong, B and Zhang, L (2019) A PV Array Reconfiguration Algorithm for Minimising Partial Shading Effects. In: Proceedings of IREC 2019: 10th International Renewable Energy Congress. IREC 2019: 10th International Renewable Energy Congress, 26-28 Mar 2019, Sousse, Tunisia. IEEE . ISBN 978-1-7281-0140-8

https://doi.org/10.1109/IREC.2019.8754602

A PV Array Reconfiguration Algorithm for Minimising Partial Shading Effects

Mohamed Etarhouni, Benjamin Chong, Li Zhang
School of Electrical and Electronic Engineering, University of Leeds
Woodhouse lane, Leeds, LS2 9JT, UK
fy09mse@leeds.ac.uk, b.chong@leeds.ac.uk, l.zhang@leeds.ac.uk

Abstract— A photovoltaic array is subject to reduction of output caused by partial shading which causes bypass diodes to turn on. This can be alleviated by partly or fully cross-tying the modules within the rows of the array, and reconfiguring the positions of modules within it. In this paper a PV array reconfiguration algorithm based on a magic square is proposed. The **reconfigured array** has **the shading effects more evenly dispersed over the entire array surface,** which **reduces voltage** and c**urrent drop due to** the diode conduction. T**he performance of this scheme** is assessed using simple models of shading patterns, and compares favourably with results from **Futoshiki and PRM-FEC algorithms**, and a conventional totally cross-tied (TCT) array, **under most of the chosen shading patterns.**

I. INTRODUCTION

The impact of partial shading on the output power of a PV array system has received considerable attention [1]. Partial shading can arise from the shadows of trees, bird's droppings, nearby buildings, passing clouds and other moving objects [2]. The problem has been addressed in many research studies [3-5]. It is found that the shading leads to a significant reduction in the total power output, along with higher losses and possibly overheating in the shaded cells.

This power reduction is independent of the shaded area, but it is influenced by several factors, such as interconnections between the array modules, shade geometry and the location of the shaded PV modules. A commonly used technique for reducing the distractive effects of electrical mismatches is to employ bypass diodes [6]; however, the main disadvantage of this is the occurrence of multiple power peaks which are dispersed widely within the operating voltage range. Another major issue with using bypass diodes is that they cannot extract all the available solar power [7, 8]. Power Electronic Equalizers including the Module Integrated Converters MICs, series and parallel schemes of Differential Power Processing DPP converters are altogether used at the sub-module level to achieve a true MPPT and enhance the total system efficiency, but these techniques can still add losses to the system as well as increasing the size and cost [9-10].

Changing the PV array interconnections is an alternative method of reducing the effects of the partial shading and increasing the output power. Series and parallel connected arrays are the conventional configurations [11], and [12] has discussed the performance of each array connection scheme in detail. The significant disadvantages of either series or parallel interconnections are that current and voltage levels are respectively lower under shading. Concerning the Series-Parallel (SP) configuration, PV panels are serially-connected to obtain the required voltage level; then they are connected in parallel to achieve the desired current level. By modifying the connections of SP, Tied-Cross-Ties (TCT) and Bridge-Linked (BL) configurations are derived through connecting ties across rows of the junction. Moreover, the most recent studies have confirmed that TCT array always shows a superior performance due to its cross ties when comparing to the conventional array configurations under Partial Shading Conditions (PSCs) [13].

A simple array such as TCT can still be modified or "reconfigured" by conceptually moving any module to a different physical location in the array, without changing any electrical connections. Although the electrical topology appears unchanged, the average array performance can clearly be changed by the statistical spatial correlations of the shading. In practice, since modules are nominally identical, reconfiguration is actually achieved by changing the interconnections. Proposed reconfiguration schemes such as that based on SuDoKu [14], a generalized algorithm proposed by [13], and others, have shown better performance than TCT in power generation under shading conditions.

This paper presents a PV array reconfiguration scheme which leads to a novel layout called Magic Square- Enhanced Configuration (MS-EC). The feature of this configuration is that the shading effects are more evenly dispersed over the entire array surface than the other schemes. In turn occurrences of terminal voltage drop due to the switching on of bypass diodes or the string current reduction due to shaded modules can be reduced. In this paper the algorithm for deriving the Magic Square (MS) from any number of squared PV arrays will be presented. The resultant MS configuration will be compared with TCT and two recent published structure; Futoshiki, [15] and PRM-FEC [16]. The results showing incresed power generation under PSC will be discussed.

II. PV ARRAY MODELLING

A practical photovoltaic (PV) array consists of a cluster of generating units or modules connected in series and/or parallel combinations. A module itself is a group of PV cells where each

is a p-n junction able to convert energy from sunlight into electricity.

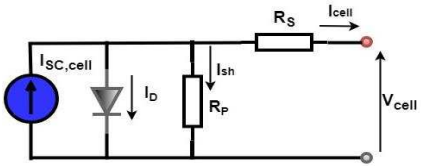

Fig.1. Equivalent circuit of a solar cell based on the single diode model

Fig. 1 shows an accepted equivalent circuit for a PV cell using a single diode model. The key element is the current source I_{SC} which is dependent on the cell temperature and the light intensity level, and can be expressed as:

$$I_{SC} = \left[I_{SCr} + K_i(T_C - T_{ref})\frac{G_K}{G_0}\right] \quad (1)$$

where I_{SCr} is the short circuit current at a given reference temperature, K_i is the temperature coefficient of the short circuit current, T_{ref} is the cell reference temperature, G_K is the actual solar irradiance of a PV cell in W/m^2 and G_0 = 1000 W/m^2 is the nominal solar irradiance under standard conditions. The other two main elements of the circuit model are the internal resistances R_S and R_P which characterise the operating conditions under which there is power loss in the semiconductor material and current leakage through the p-n junction. Thus, the output current of a single cell is given by

$$I = I_{SC} - I_O\left[\exp\left(\frac{q}{KT_CA}(V + IR_S)\right) - 1\right] - \frac{V+IR_S}{R_P} \quad (2)$$

where I_O is the reverse saturation current which refers to the leakage current, T_C is the cell temperature in kelvin (K), k is Boltzmann's constant (K=1.38×10^{-23} J/K), q is the charge of the electron (q=1.6×10^{-19} C), and A is the ideality factor. The above mathematical model can be extended to consider a group of cells connected in series and parallel. Thus, the electrical characteristics of a PV module can be simulated and are shown in Fig 2.

Figs. 2(a) and (b) respectively show the I-V and P-V characteristics of a PV module under various weather conditions. The short-circuit current (i.e. at zero voltage) is observed to be proportional to the solar irradiance while the open-circuit terminal voltage (i.e. at zero current) changes with an increase in temperature. However, varying the intensity levels widely leads to a very small effect on the voltage at which the maximum power point occurs whereas an increase in temperature can change this voltage more significantly.

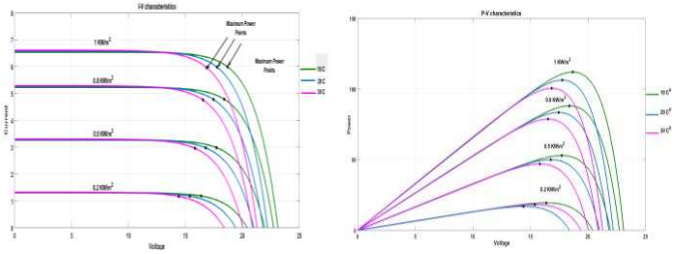

(a) (b)

Fig.2. Electrical characteristics of a PV cell (a) I-V curves; (b) P-V curves

III. Mathematical Representation of the Conventional PV Array Interconnections

The PV modules of an array are connected in series and parallel to achieve practical levels of voltage and current at the array terminals. The key approach for evaluating several array configurations under different PSCs is through the analysis of variations in the voltage, current and power of the conventional array interconnections either series, parallel or both [11]. To illustrate this approach, the output behaviour of a PV array having K number of modules is analysed under non-uniform irradiation conditions. When each module is operating independently from others (e.g., it is used as a single generating unit for a load), it is able to generate maximum power at a current I_m and voltage V_m. Before this approach is thoroughly explored, the simplest cases of PV array being irradiated with uniform irradiation are considered initially. Then for series and parallel connections, the total current and voltage are (I_m, KV_m) or (KI_m, V_m) respectively and the total power in either case is $KV_m I_m$ [13]. The same approach to quantifying the power can still be applied for combinations of series and parallel connection of modules such as those illustrated in Fig. 3 where the SP along with TCT and BL array configurations have a number of rows (m) and a number of columns (n), each column being a series string. Under uniform illumination the result is clearly unaffected by arbitray cross linkings of the columns made within the same row; the total number of modules is still $K = m \times n$ and the current, voltage and power equations can be written respectively as

$$I_{Array} = nI_m, \quad V_{Array} = mV_m$$

and

$$P_{Array} = (m \times n)I_m V_m = KI_m V_m \quad (3)$$

If the power output of a module under standard weather conditions or its rated power is defined as P_{rated}, the array power can be assumed to be varying proportionally with the shading level $S = \frac{G_K}{G_0}$ and the power expression in Equation (3) can be re-written as

$$P_{Array} = SKP_{rated} \quad (4)$$

where $I_m V_m = SP_{rated}$.

This situation is more complicated when the PV modules are non-uniformly shaded. Assuming that Y represents the number of modules having lower irradiation levels (or shaded modules), consider firstly the series only connection. Assuming the MPP voltage remains the same at V_m for all irradiation conditions, the MPP current of each module decreases to SI_m whereas for the unshaded modules it is still at I_m. In this connection, it is quite common to have by pass diodes across each module and therefore two simple operating conditions exist. The first operation is applied when the array terminal current is set equal to SI_m, and the bypass diodes of the shaded modules are not activated. This results in the array power expressed as

$$P_{Array} = SKI_m V_m \quad (5)$$

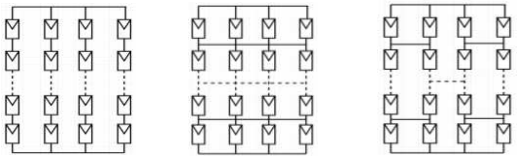

(a) (b) (c)

Fig.3. Different array configurations (a) SP; (b) TCT; (c) BL

The second method of operation is applied when the array terminal current is equal to I_m, and the bypass diodes of the shaded modules are activated resulting in a drop in the array voltage such that

$$V_{Array} = (K - Y)V_m + YV_D \quad (6)$$

Since the voltage across the diode V_D is neglected, the array power can be approximated to

$$P_{Array} = (K - Y)I_m V_m \quad (7)$$

Note that usually there is a power converter scheme at the array terminal to control the operation such that the terminal current can be either SI_m or I_m, depending on the magnitude of Equation (5) or (7). Also, there are multiple peaks on the P-V curve of the array as seen in both equations (5) and (7) respectively.

However, a similar analysis of an array having only parallel-connected PV modules shows that the P-V curve of the array only exhibits a single power peak given by

$$P_{Array} = I_{string}V_{array} = (YSI_m + (K - Y)I_m) \times V_m \quad (8)$$

where

$$I_{String} = I_{m1} + I_{m2} + \cdots + I_{mK} = (YSI_m + (K - Y)I_m)$$

and $$V_{Array} = V_m$$

It can also be observed that if the above two cases (only series and only parallel connections) have the same K, Y and S values, a parallel configuration is always resilient to the shading effects by having higher P_{Array} with a single power peak. Nevertheless, the major drawback for the parallel connection is the lower V_{Array} which is undesirable for transformer-less grid connection of the array. SP and BL configurations as illustrated in Fig. 3 may be the solution, but they may still be affected by major power drop due to non-uniform irradiation among the modules of a single series string. TCT is still considered to be the best configuration in mitigating the drawbacks of SP and BL. However, studies in [13] show that the power drop may or may not occur under certain irradiation conditions. This has been the key reason for introducing the reconfiguration scheme in a PV array.

IV. The Magic Square- Enhanced configuration (MS-EC) Algorithm

In this paper, the PV array configuration is based on an enhanced scheme which adopts the principle of creating a magic square [17]. This algorithm firstly assumes that a PV array always contains a group of neighbouring modules irradiated with the same irradiation level while there is another group irradiated at a different level. Without changing their physical locations, the aim of this algorithm is to permute all these PV modules so that their shading effects are well distributed all over the area covered by them. Therefore, the likelihood of the drop in the terminal voltage due to the activated bypass diode or the limitation on the string current due to the shaded modules can be contained. This scheme only needs to be applied before a PV array is being commissioned and after the locations of the PV modules have been decided and their typical solar irradiations are known. Thus, the physical electrical connections are determined based on this scheme and will not change provided the modules' locations remain the same. The proposed algorithm has been tested successfully by the authors for square arrays, e.g. 3×3, 5×5, 7×7 etc. Using a 3x3 array as an example, this section explains the full procedure associated with the proposed algorithm which is summarised by the flowchart in Fig. 4.

A. Proposed algorithm using an example of 3× 3 PV array

Fig 5(a) shows the structure of this example of PV array where there are nine (K = 9) PV modules. Each cell of the table represents a module, and all the modules are sequentially enumerated with a unique number (i.e. 1, 2, …, and 9). Their locations in the array structure are described by the row i and column j numbers which are included at the top and left side of the table in Fig 5(a). For example, the location of PV module 6 is described by $i_6 = 2$ and $j_6 = 1$ or a coordinate of (2, 1).

The algorithm starts by determining the new location of PV module 1 by calculating its new coordinate which is defined by

$i_{1,new} = \text{int}\left[\frac{n}{2}\right]$ and $j_{1,new} = n - 1$

where n is $\sqrt{K} = 3$ and thus, it is located at $(1, 2)$.

The new location of the subsequent PV modules will be determined by using the location of the other PV modules. For example, the new coordinate of PV module p is determined by

$i_{p,new} = i_{p-1} - 1$ and $j_{p,new} = j_{p-1} + 1$

after knowing the location of previous PV module p-1.

However sometimes, $i_{p,new}$ or $j_{p,new}$ becomes more than 2 or less than 0, and the updating formulae have to be changed according to the following conditions:

- If $i_{p,new} = -1$, then it is reset to $i_{p,new} = n - 1$.
- If $j_{p,new} = n$, then it is reset to $j_{p,new} = 0$.
- If the obtained position is occupied, the new coordinate is re-determined by
  $i_{p,new} = i_{p,new} + 1$, $j_{p,new} = j_{p,new} - 2$.
- If the obtained position is at (-1, n), then the new location is reset to (0, n – 2).

The new arrangement of this example 3 × 3 array with the above shuffling technique is shown in Fig. 5(b). It can be noticed that all locations of PV panels are rearranged, unlike the previously proposed algorithms where positions of PV panels within the first column is normally fixed.

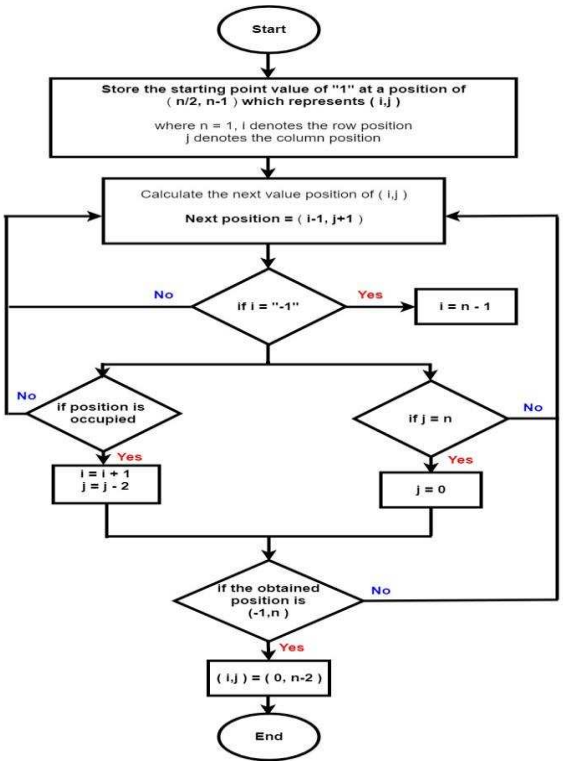

Fig.4. Flowchart of the MS-EC algorithm

As highlighted in previous section, the re-arranged structure has also revealed that the previously co-located PV modules (in Fig. 5(a) are now more distanced from each other (in Fig. 5(b)); in particular, the distance is more obvious between PV modules 1 and 2 as well as those of 8 and 9. Similar algorithm can be written for 5×5 and 7×7 PV arrays and they are optimally reconfigured as shown in Fig. 6. Again the co-located PV modules are now distanced from each other in the circuit connections.

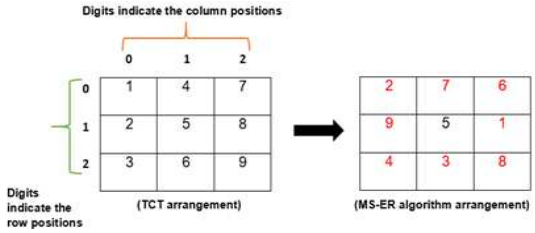

(a) (b)

Fig.5. Derivation of the MS-EC arrangement for 3×3 array (a) TCT arrangement; (b) MS-EC arrangement

9	3	22	16	15
2	21	20	14	8
25	19	13	7	1
18	12	6	5	24
11	10	4	23	17

20	12	4	45	37	29	28
11	3	44	36	35	27	19
2	43	42	34	26	18	10
49	41	33	25	17	9	1
40	32	24	16	8	7	48
31	23	15	14	6	47	39
22	21	13	5	46	38	30

(a) (b)

Fig.6. Derivation of the MS-EC arrangement for (a) 5×5 array; (b) 7×7 array

B. Various shading condition patterns

In order to validate the proposed algorithm, a comprehensive investigations were made on the MS-EC arrangement algorithm based on four common patterns of partial shading, where PV modules receive inconsistent insolation levels as seen in Fig. 7. These shading types are categorised depending on the number of shaded columns within the array (narrow or wide) and the number of shaded modules in a string; namely Short-Narrow (SN), Short-Wide (SW), Long-Narrow (LN) and Long-Wide (LW). The simulation study was accomplished using MATLAB/Simulink software, and the corresponding PV module specifications are tabulated in Table 1.

TABLE 1. PV module specifications

Maximum Power P_{max}	**106.2468 W**
Open Circuit Voltage V_{oc}	**22.17 V**
Voltage at MPP V_m	**17.77 V**
Short Circuit Current I_{sc}	**6.573 A**
Current at MPP I_m	**5.979 A**
Number of cells in series	**42**

A useful example of short-wide (SW) shading as shown in Fig.7 i (b) is used to analytically validate the superior performance of the square algorithm when compared to the conventional TCT configuration. A mathematical expressions of the current of each row along with the total power are expressed for both TCT and MS-EC configurations respectively under this shading condition.

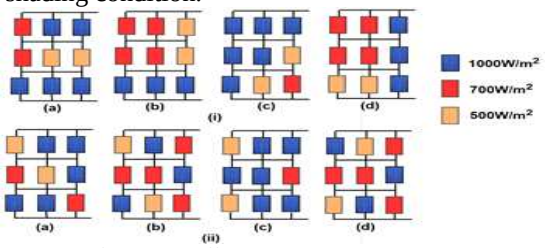

Fig.7. Distribution of the shade effect (i) TCT arrangement; (ii) MS-EC arrangement; (a) short-narrow; (b) short-wide; (c) long-narrow; (d) long-wide

The current flowing through any row of the TCT array connections is given by the following expression:

$$I_{Row} = \sum_{K=1}^{m} \frac{G_K}{G_0} I_m \tag{9}$$

where m is the number of panels in a particular row. Additionally, the PV array voltage is expressed as:

$$V_{Array} = \sum_{K=1}^{n} V_{mK} \tag{10}$$

where, n is the number of rows connected in parallel within the array. Thus, the total array power is given by:

$$P_{Array} = \sum_{K=1}^{n} \sum_{K=1}^{m} \frac{G_K}{G_0} I_m V_{mK} = \sum_{K=1}^{m \times n} \frac{G_K}{G_0} I_m V_{mK} \tag{11}$$

The current of the individual rows in the TCT configuration are calculated as follows:

$$I_{Row1} = I_{Row2} = 0.7I_m + 0.7I_m + 0.5I_m = 1.9I_m \text{ (A)}$$

$$I_{Row3} = 3I_m \text{ (A)}$$

TABLE 2. Row currents of TCT and MS-EC configurations under PSCs

Shading pattern	Row currents of TCT			Row currents of MS-EC		
	I_{R1}	I_{R2}	I_{R3}	I_{R1}	I_{R2}	I_{R3}
SN	$2.7I_m$	$1.7I_m$	$3I_m$	$2.5I_m$	$2.2I_m$	$2.7I_m$
SW	$1.9I_m$	$1.9I_m$	$3I_m$	$2.2I_m$	$2.4I_m$	$2.2I_m$
LN	$3I_m$	$2.5I_m$	$2.2I_m$	$2.5I_m$	$2.7I_m$	$2.5I_m$
LW	$2.4I_m$	$2.4I_m$	$2I_m$	$2.2I_m$	$2.4I_m$	$2.2I_m$

V. Results and Discussions

Following the above analysis, the theoretical values of the row currents for TCT and the proposed MS-EC arrangements are altogether summarised in Table 2 under the four mentioned shading patterns as seen in Fig.7. Besides, the location of Global Maximum Power Points G_{MPP} based on theoretical and simulated values are also compared and verified for both TCT and the proposed algorithm arrangements respectively as depicted in Table 3. The power enhancement due to the MS-EC algorithm is calculated in Table 3 and expressed by:

$$\%P_{Improvement} = \frac{P_{MS-EC} - P_{TCT}}{P_{TCT}} \times 100 \qquad (12)$$

Where $P_{MS\text{-}EC}$, P_{TCT} both represent the power generated by the proposed algorithm and TCT arrangements under a particular shading condition.

A. Short-Narrow shading pattern (SN)

According to the above mathematical analysis, MS-EC was observed to increase output power from $5.4I_mV_m$ to $6.6I_mV_m$ under SN shading when compared to the conventional TCT arrangement. As a consequence of MS-EC algorithm, it was able to achieve a better arrangement of PV modules where the solar irradiance equalisation is performed to reduce the losses and increase the incoming current through the nodes. The power improvement based on the theoretical and simulation analysis by the proposed algorithm when compared to TCT is significant as seen in Table 3 below.

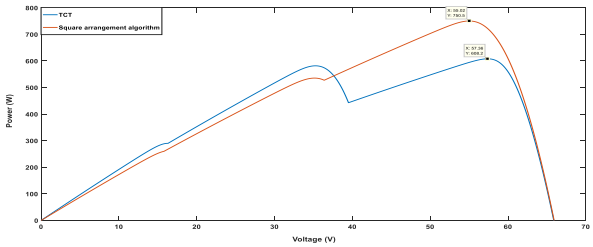

Fig.8. P-V curve for TCT and MS-EC under SN shading

B. Short-Wide shading pattern (SW)

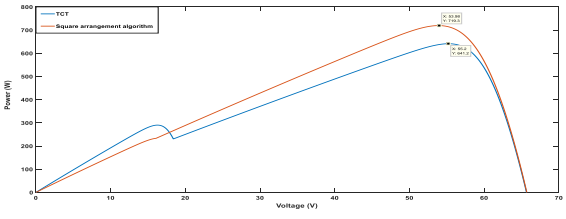

Fig.9. P-V curve for TCT and MS-EC under SW shading

According to Fig.7 (b), two rows are heavily shaded with shading levels of 0.7 and 0.5 respectively within the TCT connection. MS-EC was found to improve the global maximum power from $6I_mV_m$ to $6.6I_mV_m$ by facilitating a better shade distribution. On average, MS-EC increased the global power by 10% theoretically when compared to TCT. Moreover, the MS-EC showed a higher power performance (719.4W) than that of the TCT (641.2W).

C. Long-Narrow shading pattern (LN)

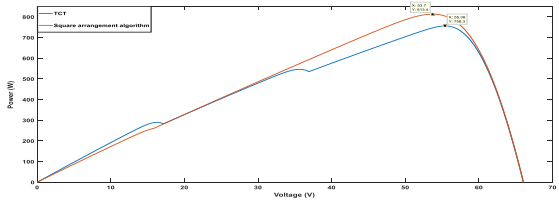

Fig.10. P-V curve for TCT and MS-EC under LN shading

Theoretical analysis revealed that MS-EC showed the highest G_{MPP} of $7.5I_mV_m$, thus presenting only a single power peak under this pattern. Therefore, the MS-EC increased the power theoretically to 13.63% compared to the TCT configuration. As seen in Fig. 10, the simulated power produced by the proposed algorithm is higher than that of TCT under LN pattern; hence MS-EC improved the total power by 7.55% when comparing to TCT.

D. Long-Wide shading pattern (LW)

Analytical expressions for the global power of both MS-EC and TCT configurations were observed to show a similar performance of $6.6I_mV_m$ and $6I_mV_m$ respectively. In addition, MS-ER presented two power peaks on the P-V curve while TCT showed three power peaks according to theoretical results. Simulation results in Fig.11 revealed that MS-EC generated a global power peak at 719.4W whereas TCT produced 686.1W under this shading pattern. Overall, MS-EC raised the output power by 4.85% in relation with the simulation results as presented in Table 3.

On extensive study, another comparison was carried out on 5×5 array size between the MS-EC algorithm and other two existing algorithms; namely Futoshiki, [15] and PRM-FEC, [16] respectively. Table 4 presents the summary of the results for the maximum power generated by these mentioned algorithms as well as the traditional TCT under various shading patterns as seen in Fig. 12.

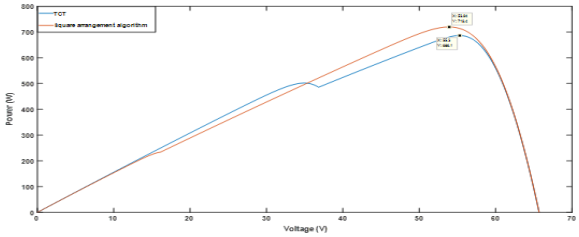

Fig.11. P-V curve for TCT and MS-EC under LW shading

TABLE 3. Theoretical and Simulated G_{MPP} values for TCT and MS-EC under various shading conditions

Shading Pattern	**TCT Location of G_{MPP}**		**MS-EC Location of G_{MPP}**		**%Improved power**	
	$P_{Theoretical}$ (W)	$P_{Simulated}$ (W)	$P_{Theoretical}$ (W)	$P_{Simulated}$ (W)	$P_{Theoretical}$ (W)	$P_{Simulated}$ (W)
SN	$5.4I_mV_m$	608.2	$\mathbf{6.6I_mV_m}$	**750.5**	22.2	23.97
SW	$6I_mV_m$	641.2	$\mathbf{6.6I_mV_m}$	**719.4**	10	12.30
LN	$6.6I_mV_m$	756.3	$\mathbf{7.5I_mV_m}$	**813.4**	13.63	7.55
LW	$6I_mV_m$	686.1	$\mathbf{6.6I_mV_m}$	**719.4**	10	4.85

TABLE 4. Maximum generated power of different algorithm arrangements along with the conventional TCT under PSCs

Shading Type	TCT P_{max} (W)	MS-EC P_{max}(W)	Futoshiki P_{max} (W)	PRM-FEC P_{max} (W)
SN	2257	**2352**	**2352**	**2353**
SW	1533	**1958**	1902	**1958**
LN	1365	**1790**	1723	1723
LW	1468	**1598**	1579	1579
Centre	1732	**2098**	2044	2044
Progressive	2090	**2199**	2043	2043

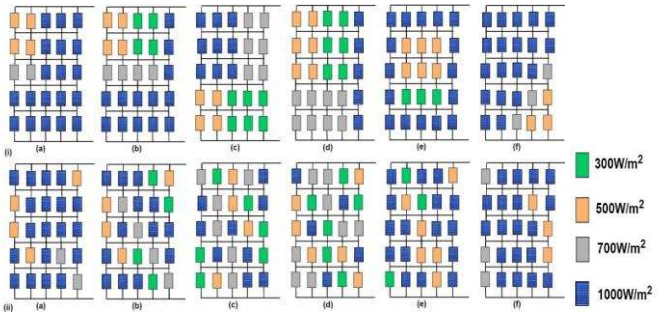

Fig.12. Distribution of the shading effect based on different patterns in (i) normal TCT arrangement (ii) MS-ER arrangement (a) SN; (b); SW; (c) LN; (d) LW; (e) Centre; (f) progressive

VI. CONCLUSION

In summary, the obtained results show that the square arrangement algorithm has led to a substantial improvement in the output power by **27.72%** and **31.13%** when compared to TCT, under short-wide and long-wide shading patterns respectively. Moreover, the proposed algorithm was compared with Futoshiki and PRM-FEC algorithms, and it was shown that both of the latter yielded less power than that of the square algorithm under most of the chosen shading patterns. These performance improvements can be obtained with only a fixed change to the array interconnections, made during manufacture or installation.

REFERENCES

[1] A. Dolara, G. C. Lazaroiu, S. Leva, and G. Manzolini, "Experimental investigation of partial shading scenarios on PV (photovoltaic) modules," Energy, vol. 55, pp.2013.

[2] S. Mohammadnejad, A. Khalafi, and S. M. Ahmadi, "Mathematical analysis of total-cross-tied photovoltaic array under partial shading condition and its comparison with other configurations," Solar Energy, vol. 133, pp. 501-511, 2016.

[3] H. Ziar, M. Nouri, B. Asaei, and S. Farhangi, "Analysis of Overcurrent Occurrence in Photovoltaic Modules With Overlapped By-Pass Diodes at Partial Shading," IEEE Journal of Photovoltaics, vol. 4, pp. 713-721, 2016.

[4] M. C. Di Vincenzo and D. Infield, "Detailed PV array model for non-uniform irradiance and its validation against experimental data," Solar Energy, vol. 97, pp. 314-331, 2015.

[5] A. Dolara, G. C. Lazaroiu, S. Leva, and G. Manzolini, "Experimental investigation of partial shading scenarios on PV (photovoltaic) modules," Energy, vol. 55, pp.2015.

[6] H. S. Sahu, S. K. Nayak, and S. Mishra, "Maximizing the Power Generation of a Partially Shaded PV Array," IEEE Journal of Emerging and Selected Topics in Power Electronics, vol. 4, pp. 626-637, 2016.M. Young, The Technical Writer's Handbook. Mill Valley, CA: University Scienc

[7] E. V. Paraskevadaki and S. A. Papathanassiou, "Evaluation of MPP Voltage and Power of mc-Si PV Modules in Partial Shading Conditions," IEEE Transactions on Energy Conversion, vol. 26, pp. 923-932, 2011.

[8] H. Kawamura, K. Naka, N. Yonekura, S. Yamanaka, H. Kawamura, H. Ohno, et al., "Simulation of I–V characteristics of a PV module with shaded PV cells," Solar Energy Materials and Solar Cells, vol. 75, pp. 613-621,2015.

[9] G. R. Walker and J. C. Pierce, "Photovoltaic DC-DC module integrated converter for novel cascaded and bypass grid connection topologies — Design and optimization," in 2006 37th IEEE Power Electronics Specialists Conference, 2006, pp. 1-7.

[10] H. Lee and K. A. Kim, "Differential power processing converter design for photovoltaic wearable applications," in 2016 IEEE 8th International Power Electronics and Motion Control Conference (IPEMC-ECCE Asia), 2016, pp. 463-468.

[11] R. Ramaprabha and B. L. Mathur, "A Comprehensive Review and Analysis of Solar Photovoltaic Array Configurations under Partial Shaded Conditions," International Journal of Photoenergy, 2017.

[12] L. Gao, R. A. Dougal, S. Liu, and A. P. Iotova, "Parallel-Connected Solar PV System to Address Partial and Rapidly Fluctuating Shadow Conditions," IEEE Transactions on Industrial Electronics, vol. 56, pp. 1548-1556, 2016.

[13] S. Malathy and R. Ramaprabha, "A static PV array architecture to enhance power generation under partial shaded conditions," in 2015 IEEE 11th International Conference on Power Electronics and Drive Systems, 2015, pp. 341-346.

[14] M. Horoufiany and R. Ghandehari, "Optimization of the Sudoku based reconfiguration technique for PV arrays power enhancement under mutual shading conditions," Solar Energy, 2018, vol. 159, pp. 1037-1046.

[15] H. S. Sahu, S. K. Nayak, and S. Mishra, "Maximizing the Power Generation of a Partially Shaded PV Array," IEEE Journal of Emerging and Selected Topics in Power Electronics, vol. 4, pp. 626-637, 2016.

[16] V. Darmini and K. Sunitha, "Comparison of solar PV array configuration methods under different shading patterns," in 2017 International Conference on Technological Advancements in Power and Energy (TAP Energy), 2017, pp. 1-4.

[17] N. Rakesh, T. V. Madhavaram, K. Ajith, G. R. Naik, and P. N. Reddy, "A new technique to enhance output power from solar PV array under different partial shaded conditions," in 2015 IEEE International Conference on Electron Devices and Solid-State Circuits (EDSSC), 2015, pp. 345-348.